*Atmosfera (1998) **11**, pp. 11-28*

Study of a cyclone wave in the Drake Passage region

SILVINA A. SOLMAN

Centro de Investigaciones del Mar y la Atmósfera (CIMA) Consejo Nacional de Investigaciones Científicas y Técnicas (CONICET), y Depto. De Cs. de la Atmósfera, Univ. de Bs. Aires, Buenos Aires, Argentina

CLAUDIO G. MENÉNDEZ

Centro de Investigaciones del Mar y la Atmósfera (CIMA) Consejo Nacional de Investigaciones Científicas y Técnicas (CONICET),

(Manuscript received Oct. 25, 1996; accepted in final form May 12, 1997)

RESUMEN

Se examinó la evolución de un sistema de cuña-vaguada ocurrido en la periferia antártica a fines de julio de 1986. Una perturbación ciclónica se desarrolló en el flanco polar de un anticiclón de bloqueo dando lugar a un profundo ciclón al este del Pasaje de Drake. La madurez y el decaimiento del sistema tuvo lugar en el Mar de Weddell, en una región ciclolítica de acuerdo con la climatología. Se evaluó el balance de energía cinética de las perturbaciones usando análisis del ECMWF cada 12 horas. Se puso énfasis en el rol del proceso de desarrollo baroclínico corriente abajo durante el crecimiento y decaimiento de los centros de energía asociados con la onda ciclónica.

El crecimiento inicial de un centro de energía cinética cerca de 90°O fue dominado por la convergencia de los flujos ageostróficos de geopotencial, originados en un centro de energía previo, en estado de disipación. La conversión baroclínica resultó poco relevante debido a la baja baroclinicidad en esa región. Al intensificarse este centro de energía, comenzó a exportar energía corriente abajo, hacia el este del Pasaje de Drake, donde se desarrolló un profundo ciclón, con un nuevo centro de energía cinética asociado. Se encontró que los flujos ageostróficos de geopotencial y, en menor medida, la conversión baroclínica, fueron los procesos físicos más importantes durante la etapa inicial de crecimiento. Finalmente, este último centro de energía comenzó a decaer, principalmente, por divergencia de flujo.

ABSTRACT

The evolution of a ridge-trough system that occurred in the periphery of the Antarctic in late July 1986 is examined. A cyclonic disturbance within the polarward side of a blocking anticyclone, developed into an intense closed circulation to the east of the Drake Passage. The maturity and decay of the system took place over the Weddell Sea, a location for cyclolysis according to the climatology. The eddy kinetic energy budget of this wave was evaluated, using 12-h ECMWF operational analyses, in order to identify the physical processes that contributed to its development. Particularly, attention was given to the role of the downstream baroclinic development process in the growth and decay of energy centers associated with the cyclonic wave.

The initial growth of an eddy kinetic energy center near 90°W was mastered by the convergence of ageostrophic geopotential fluxes, originated from a previous energy center in dissipation stage. The center developed in a region of relatively low baroclinicity and then the incidence of the baroclinic conversion process was not significant. As the center intensified, it produced strong radiation of energy downstream to the east of Drake Passage, where a deep cyclone developed, with a new associated eddy kinetic energy center. It was found that the convergence of ageostrophic geopotential fluxes and, in lesser extent, the baroclinic conversion were the most important physical processes during the early stage of growing. Finally, this last energy center decayed, mainly, by flux divergence.

1. Introduction

Over the past fifty years, a large number of studies have been compiled regarding the life cycle of extratropical cyclones in which baroclinic growth and barotropic decay were the main processes involved. Only recently it has been possible to confirm, using observational data and numerical simulations, the existence of downstream development as an important mechanism in the life cycle of mid-latitudes cyclonic systems. Orlanski and Katzfey (1991) and Orlanski and Sheldon (1993) (hereafter O&K and O&S, respectively) have demonstrated, in analyzing the development of cyclonic systems in the Southern and Northern Hemisphere, respectively, that the downstream radiation of energy and the local baroclinic conversion can be quite important in the development of extratropical cyclones.

Complementary work using idealized simulations (Simmons and Hoskins, 1979, Orlanski and Chang, 1993 and Chang and Orlanski, 1993) pointed out the mechanism in which downstream radiation of ageostrophic geopotential fluxes by an upstream eddy acts as a trigger for the development of downstream cyclones over less baroclinic zones. This process has been defined as Downstream Baroclinic Development (DBD) and refers to the process of dispersion and spreading of energy in a growing unstable system, characteristic of baroclinic waves (Orlanski and Chang, 1993).

Earlier observational studies, such as Namias and Clapp (1944), Cressman (1948), Hovmöller (1949) and Joung and Hitchman (1982) discussed specific examples of downstream effects in the development of storms for the Northern Hemisphere, but it was found ubiquitous in the Southern Hemisphere, as pointed out by van Loon (1965) and Trenberth (1986).

Based on regression analysis for 7 winter seasons using European Centre for Medium-Range Weather Forecasts (ECMWF) data, Chang (1993) demonstrated that DBD is a dominant process in much of the northern Pacific storm track. More recently, Berbery and Vera (1996) applied a similar technique to 6 winter seasons using ECMWF data for the Southern Hemisphere (hereafter, SH) and found that in the Pacific storm track the DBD played a major role in eddy generation.

Our main interest is focused in the area around the Antarctic Peninsula and southern South America. The eastern South Pacific Ocean is unique in that winter cyclogenesis occurs within two well-defined zones at middle and high latitudes. The mean cyclogenetic zone at high latitudes is located west of Drake Passage, downstream of the polar branch of the westerlies (Carleton, 1981). A detailed climatology of cyclone frequency near the Drake Passage based on a 22-year of daily synoptic charts is presented by Mayes (1985) who found two important cyclone tracks at around 55°S and 64°S. He also showed that the area off the northeast coast of the Antarctic Peninsula is particularly cyclogenetic in winter. The pattern of the cyclonic activity in the SH shows a general south-eastward motion of vortices with maturity and cyclolysis over the Antarctic oceans. However, cyclonic vortices developed south-west of South America frequently travelled to the north-east and passed through Drake Passage, or across the Antarctic Peninsula; they are usually by then in a decaying phase. Over the western South Atlantic Ocean, northeastward of Drake Passage, additional winter maximum of cyclone density extend along 45°-60°S (Sinclair, 1994), with frequent tracks extending southeastward to a decay region in the Antarctic trough.

The midlatitudes are characterized by an alternation of the flow regime between a relatively zonal flow and a more meridional flow with near stationary disturbances (blocking anticyclones). According to Leighton (1994) the greater part of the South Pacific Ocean could be considered a potential region for the occurrence of blocking patterns. The wintertime anticyclones that are centered near 50°S across the eastern South Pacific tend to be slow

moving, particularly those centers that develop in ridges extending from the Antarctic near the Drake Passage region and near 100°-120°W. These long-lasting blocking episodes may produce extreme weather conditions over southern South America, such as droughts (Alessandro and Lichtenstein, 1996) or large rainstorms (Garreaud, 1994).

Our interest is to study the behavior of high frequency transient eddies interacting with a blocking anticyclone. The life cycle of a ridge-trough system is analyzed here with the main purpose of inquiring into the mechanisms that control its growth and decay. In late July 1986 a blocking event over the eastern South Pacific Ocean is followed by the development of a large trough over the Drake Passage. A deep cyclone develops further downstream over the South Atlantic Ocean at the later time. There are several plausible hypotheses explaining the behavior of this cyclone wave, one of which is downstream development, so that quantitative diagnosis is required for the resolution of the role of downstream development in the region. This ridge-trough system begins its development in the exit region of the southern Pacific storm track, where strong downstream geopotential fluxes exist (Berbery and Vera, 1996) and the mechanism of downstream development is expected to be important. The interpretation and understanding of the mechanisms operating throughout the life cycle of cyclones based on the analysis of the eddy energy budget has proven to be a very useful diagnostic tool for identifying the role of the different processes in the generation and decay of cyclonic systems.

The data used and the choice of the case study are presented in section 2. The synoptic evolution and characteristics of the cyclone event are described in section 3. Section 4 provides the evaluation of the regional energetics and the energy budget. The summary and conclusions are presented in section 5.

2. The case study: general remarks

The data set consists of twice daily ECMWF analyses on a 2.5°x 2.5° latitude-longitude grid for the six winters 1983/88. The winter SH season is defined to be the period from 1 June through 31 August. Figure 1a shows the 300-hPa wind variance averaged over the six winter seasons. In computing this variance, interannual variability has been removed by subtracting from the series the seasonal mean for each season. The meridional wind perturbation was used as it represents adequately cyclonic waves (Chang, 1993). The storm track maxima (i.e., areas where the variance is largest) are found near the date line at about 60°S and along 30°-35°S. Minimum values are found over the Pacific Ocean at about 100°-120°W and near New Zealand.

In order to identify persistent anomalies associated with blocking highs and broad ridges through the data set a threshold criterion were used. We define persistent anomalies to be 500-hPa height anomalies at a given grid point larger than 100 m which persist longer than 5 days. The grid point 57.5°S, 92.5°W was chosen because persistent anomalies were frequent there. We have found eight events spanning 72.5 days. Figure 1b shows the variance of 300-hPa meridional wind averaged over the 72.5 days which correspond to the occurrence of such persistent anomalies. We see that the variance weakens near the position of the blocks (at about 110°W). Also, there is a suggestion of enhanced variance upstream, downstream and to the northwest of the block. This enhanced high frequency variability is especially evident over the Drake Passage.

The flow regime associated with these positive persistent anomalies is analyzed in this paper for a characteristic individual case that occurred in late July 1986. The chosen case exhibits a slow moving anticyclone over the eastern South Pacific ocean followed by a deep trough in the Drake Passage region. In Figure 2, we have computed a Hovmöller or longitude-time diagram of the meridional wind perturbation, v', averaged over a latitude band, for part of the 1986 winter season. Since the latitudinal position of the eddy maximum varies quite a bit in

time, the latitudinal band over which the average was done is 45°-75°S, centered with the subpolar jet stream. (Tests were done by changing the latitudinal extension of the latitudinal band being averaged with similar results as those presented here). The analyses were done at 300 hPa for the period from 15 July through 14 August. A Hovmöller of v'^2 is also included because it sometimes allows the wave packets to be more easily identified. Several wave groups can be identified propagating across the Pacific Ocean, but it is noticeable a wave group emanating from the entrance of the subpolar jet stream in the Atlantic Ocean by 20 July (near 30°E), that propagates across the Pacific and decays at the southwestern Indian Ocean (50°E) by 4 August, circling the globe. The wave group developing eastward the dateline is the subject for this study. We will concentrate on the development of the associated ridge-trough system from 26 through 31 July.

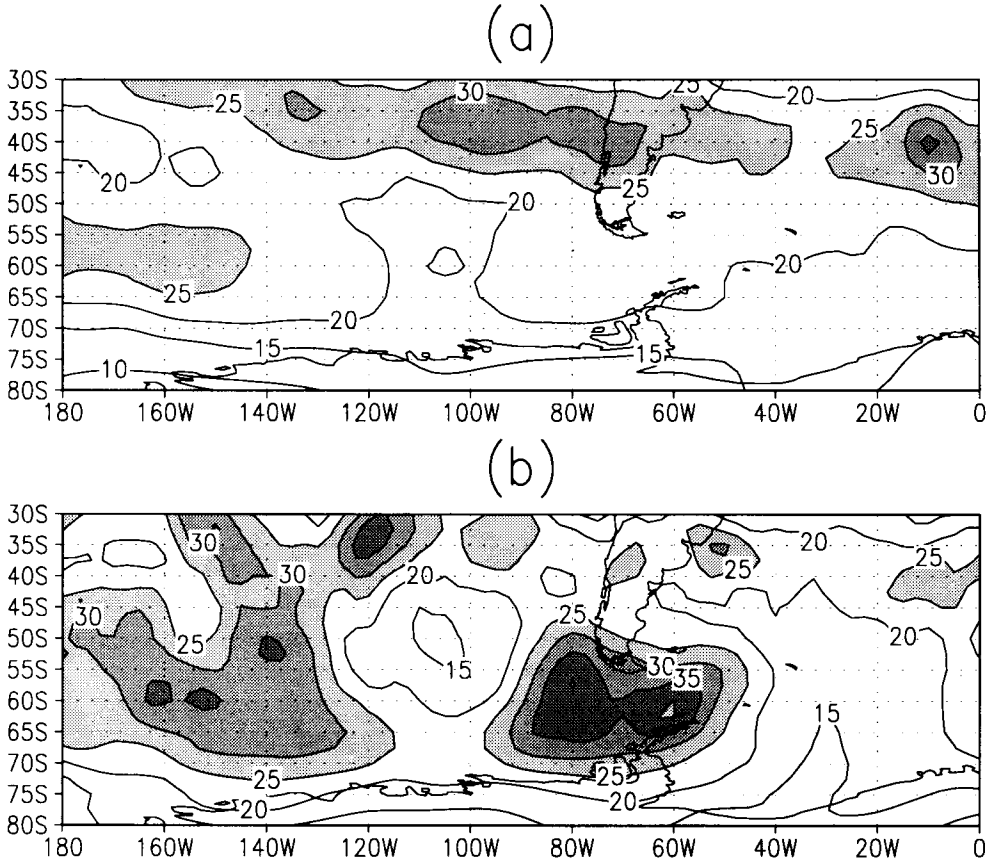

Fig. 1. (a) Variance of the 300 hPa meridional wind averaged over the six winter seasons 1983/88. Contour interval is 5x10 m^2s^{-2}, values larger than 25x10 m^2s^{-2} are shaded. (b) Same as (a) except averaged over the periods in which 500 hPa positive persistent anomalies satisfying the threshold and duration criteria of 100 m and 5 days at 57.5°S, 92.5°W were occurring.

The discussions of the selected case study are based on the data set previously mentioned. In the following, "analyses" will refer to these data. Perturbations were defined as deviations from the monthly mean. The analyses were used to diagnose the synoptic features of the developing systems (section 3) and to evaluate the most relevant terms of the kinetic energy budget (section 4).

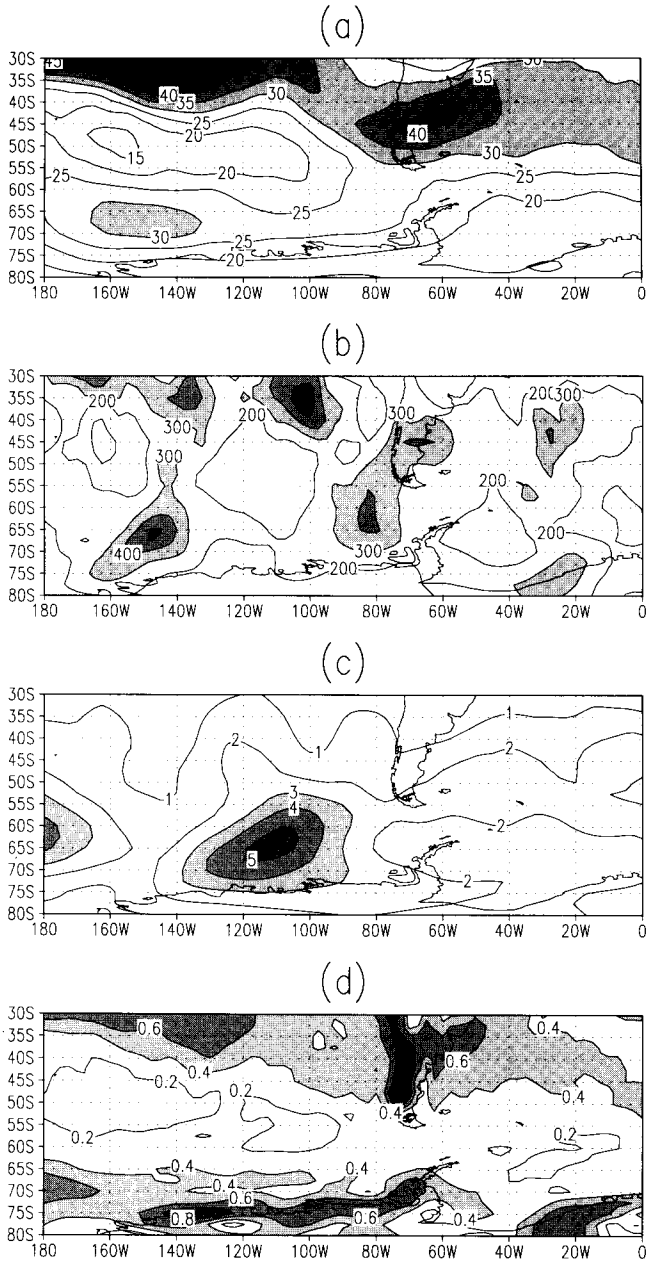

Fig. 2. Hovmöller diagrams of eddy meridional wind at 300 hPa (a) and eddy meridional wind squared (b) averaged over 45°-75°S for the period 15 July - 14 August 1986. The contour intervals are 5 ms^{-1} and 100 m^2s^{-2}. In (a), the zero contour is omitted, solid contours are positive, and dashed contours negative.

3. Synoptic description

In this section a qualitative description of the mean flow for July 1986 and a synoptic description of the ridge-trough system for the period between 26 12Z and 30 12Z are given. On the central and western Pacific Ocean is observed (Fig. 3a) the axis of the subtropical jet (STJ) at about 30°S and the axis of the polar jet (PJ) near 67°S. The dual jet structure of the westerlies, typical of the austral winters, is maintained until 100°W approximately. Eastward both jets are weakened, and the STJ is diverted southward, reaching a secondary intensity maximum over South America.

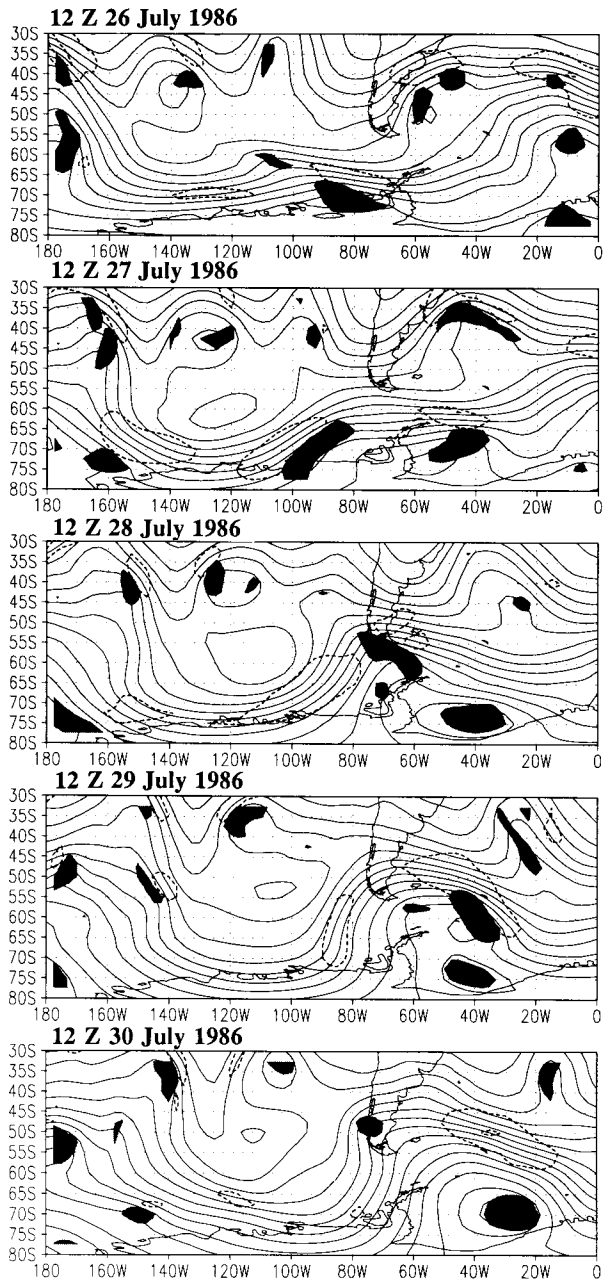

Fig. 3. (a) 300 hPa July 1986 31-day mean wind. Wind speed interval is 5 ms^{-1}, greater than 30 ms^{-1} shaded. (b) July 1986 variance of the 300 hPa meridional wind perturbations. Contour interval is 100 m^2s^{-2}, greater than 300 m^2s^{-2} shaded. (c) July 1986 variance of the 500 hPa geopotential heights. Contour interval is 10^4 m^2, greater than $3x10^4$ m^2 shaded. (d) July 1986 Eady growth rate for the 850-700 hPa layer. Contour interval is 0.2 day^{-1}, greater than 0.4 day^{-1} shaded.

Figures 3b and 3c show the variances of the 300 hPa meridional wind and of the 500 hPa geopotential height for July 1986. A distinctive feature of July 1986 is the reduced eddy activity as given by $\overline{v'^2}$ between 130°W and 100°W poleward of 45°S. The $\overline{z'^2}$ field exhibits a maximum at the same location. According to Trenberth (1986) the association of the maximum of $\overline{z'^2}$ and the minimum in $\overline{v'^2}$, in a region with a local enhancement of the split in the westerlies, is an evidence of the dominance of blocking highs or ridges over that region. By comparing the three upper panels of Figure 3, it is observed a coincidence among the maxima in the eddy activity (as shown in panel b) and the position of the jet. However, to the west of the Drake Passage, exists a maximum in $\overline{v'^2}$, downstream of the maximum in $\overline{z'^2}$, in a zone where the PJ is weakened. In order to estimate the baroclinicity for July 1986, the maximum Eady growth rate as defined by Hoskins and Valdes (1990) has been evaluated for the layer 850-700 hPa (Fig. 3d). Comparison of panels a and d indicates that baroclinicity reaches maximum values beneath the STJ and beneath the PJ. Minimum values are found over the Pacific Ocean in the region between the two branches of the jet, and over the Atlantic Ocean near 60°S. Large values are also found over Antarctica, although local distortions can appear due to the high terrain and steep slopes. Note the maximum in eddy activity at 80°W (Fig. 3b) is located in a region of relatively low low-level baroclinicity, at the end of the PJ.

Figure 4 shows the 500 hPa geopotential heights, along with main regions of cyclonic vorticity (shaded) and regions with kinetic energy greater than 600 m^2s^{-2} (dashed lines), from 26 12Z through 30 12Z. It can be noticed, as the primary large-scale feature, the development of a high at about 120°W throughout the period. A deep trough west of 160°W is present at 26 12Z, associated with a matured cyclone at high latitudes. The strong poleward flow contributes to the development of the blocking high, which increases its height up to 30 12Z.

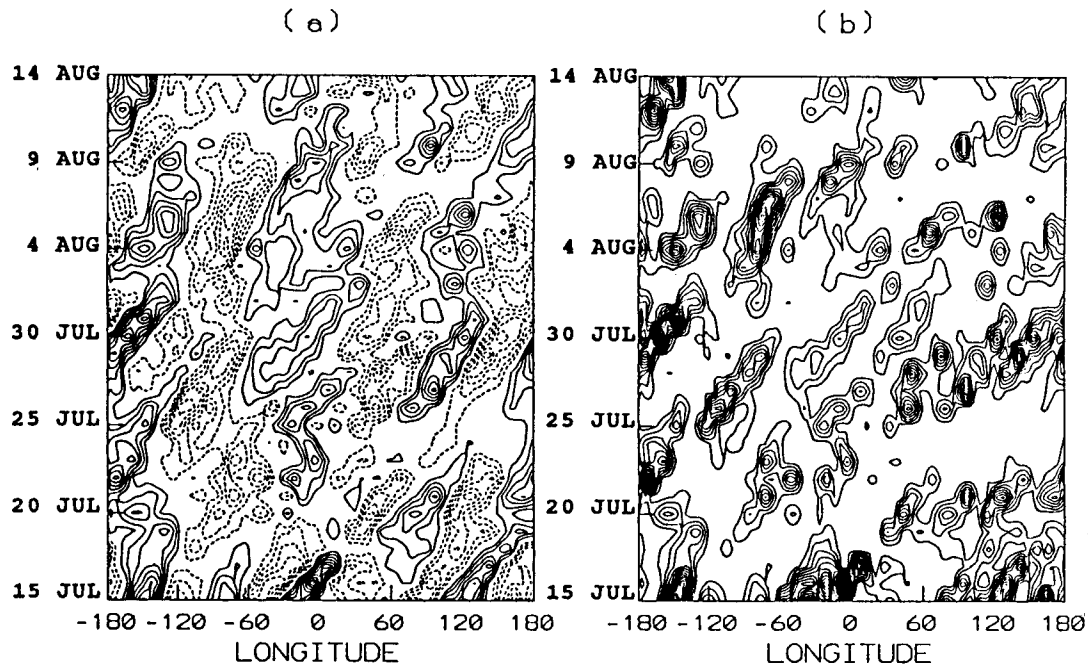

Fig. 4. 500 hPa geopotential height (solid lines, every 80 m), 500 hPa cyclonic relative vorticity (values less than $-6x10^{-5}$ s^{-1} shaded) and 500 hPa kinetic energy (dashed lines, every 600 m^2s^{-2}), at 24-h intervals from 12 Z 26 July 1986 to 12 Z 30 July 1986.

Over the eastern Pacific the cyclonic eddies are diverted to the north and south of the blocking high, following the two branches of the jet. The main features of the disturbances associated with the PJ and the STJ are rather different. At 26 12Z the high latitudes are characterized by a cyclonic system near 80°W and a smaller-scale eddy, at 62°S, 105°W. A local maximum in the kinetic energy (i.e., a jet streak) is located directly ahead of this cyclonic wave. Another jet streak propagates upstream of these systems. The STJ is more contorted with two main cyclonic systems located north of the high.

At 27 12Z the small-scale perturbation migrates eastward and merges with the cyclonic disturbance over the Bellinghausen Sea. An associated jet-streak intensifies upon arriving in southwesterly flow ahead of the ridge axis. Downstream of the Antarctic Peninsula a new cyclone develops over the Weddell Sea.

By 28 12Z a deep long-wave trough develops over the Drake Passage. Large values of cyclonic vorticity associated with the migrating disturbance, move increasingly close to that region. This trough extends from high to middle latitudes in a region where the double structure of the jets disappears. The jet streak also intensifies and extends between the ridge axis and the trough axis. The disturbance in the STJ moved southeastward and is located on the northwestern edge of the cyclonic wave. On the eastern side of the trough, the matured system over the Weddell Sea reaches its maximum depth.

By 29 12Z the trough moves eastward and occurs the subsequent intensification of the cyclone to the north of the Weddell Sea at around 62°S. At 500 hPa the circulation has closed off. This evolution is accompanied by a large increase of kinetic energy to the east of the trough base, and by a weakness of the upstream jet streak. During this time, the mature system over the Weddell Sea (at about 75°S), is losing depth and energy.

During the ensuing 24 h further intensification of the system occurs, surpassing in intensity to the previous development. The depression is moving toward the southeast, and the vorticity maximum seems to rotate around the base of the trough and becomes collocated with the circulation center. Over the Pacific Ocean, the blocking high also increases its height during this period. The intensification of the anticyclone enhances the local separation of the two jets over the region. During the next hours the cyclone becomes nearly stationary over the Weddell Sea, and begins its dissipation.

The evolution of the wave presents some similarities to that reported by Orlanski *et al.* (1991) and O&K for the explosive development of a cyclone over the Bellinghausen Sea. However, in that case the large-scale trough developed over the eastern South Pacific at around 90°W, and the upstream high was located more to the northwest with respect to our case. It is also noticeable that in Orlanski *et al.* (1991) and O&K, the anticyclone moved eastward faster (at about 12° longitude per day against about 5° longitude per day in this case).

4. Energetics

The analysis of the energy budget has proven to be a powerful tool in determining the processes that affect the development of weather systems (O&S and references mentioned therein). By properly defining a mean state, it is possible to analyze the energy transfer between an individual system and that mean state.

Following the work of O&K, eddies are defined as deviations from a time mean flow. Since we are evaluating the energy budget using data analyses, the use of a time mean (in this case, a monthly mean) is possible.

The derivation of the energy equations has been taken from O&S and the details will not be repeated here. Only a brief description of the energy equations, in which the calculations are based, is presented below.

4.1. Eddy kinetic energy equation

The energy budget is divided into a time mean (monthly mean) and an eddy part by assuming that the velocity and the thermodynamic variables can be expressed by:

$$\mathbf{V} = \mathbf{V_m} + \mathbf{v}$$

$$Q = Q_m + q$$

where **V** is the horizontal wind vector and Q is any scalar. Subscript m indicates the monthly mean and small **v** and q are the deviations from this time mean state.

The eddy kinetic energy equation in pressure coordinates is given by:

$$\frac{\partial Ke}{\partial t} = -(\mathbf{v} \bullet \nabla\phi) - \nabla \bullet (\mathbf{V}Ke) - \frac{\partial(\omega Ke)}{\partial p} - \mathbf{v} \bullet (\mathbf{v} \bullet \nabla \mathbf{V}_m) + Residue \qquad (1)$$

where $Ke=1/2\ (u^2+v^2)$, $\omega=dp/dt$ is the vertical velocity in pressure coordinates and ϕ is the geopotential height.

The term on the left represents the tendency of the eddy kinetic energy and the terms on the right are, respectively, the advection of eddy geopotential heights by the eddy velocity, the horizontal and vertical divergence of the eddy kinetic energy fluxes, and the Reynolds stresses, which, when properly averaged, could be interpreted as a transfer between mean and eddy kinetic energy, i.e., barotropic conversion of energy.

It has been demonstrated in the literature, see O&K, O&S, that $-\mathbf{v}\bullet\nabla\phi$ is the dominant source/sink term in the local eddy kinetic energy budget. O&S have proven that this term can be written as:

$$-\mathbf{v} \bullet \nabla\phi = -\nabla \bullet (\mathbf{v}\phi)_a - \omega\alpha - \frac{\partial(\omega\phi)}{\partial p} \qquad (2)$$

The first term on the right side of eq. (2) is the convergence of the ageostrophic geopotential fluxes, which represents the dispersion of energy. The second term (when volume averaged) represents the conversion from eddy potential to eddy kinetic energy and the third term is the vertical flux divergence which redistributes energy vertically via work done by pressure forces.

The ageostrophic geopotential fluxes are defined by O&S as:

$$(\mathbf{v}\phi)_a = \mathbf{v}\phi - k x \nabla \frac{\phi^2}{2f(y)} \qquad (3)$$

which are representative, averaged over an eddy, of the group velocity (O&S).

4.2. Eddy kinetic energy budget

A sequence of the vertically averaged eddy kinetic energy (50 hPa to 1000 hPa) together with the ageostrophic geopotential fluxes $(\mathbf{v}\phi)_a$, from 00Z 27 July to 12Z 30 July are depicted in Figure 5. Contours corresponding to values over 300 m^2s^{-2} are shown, in order to better identify individual energy centers.

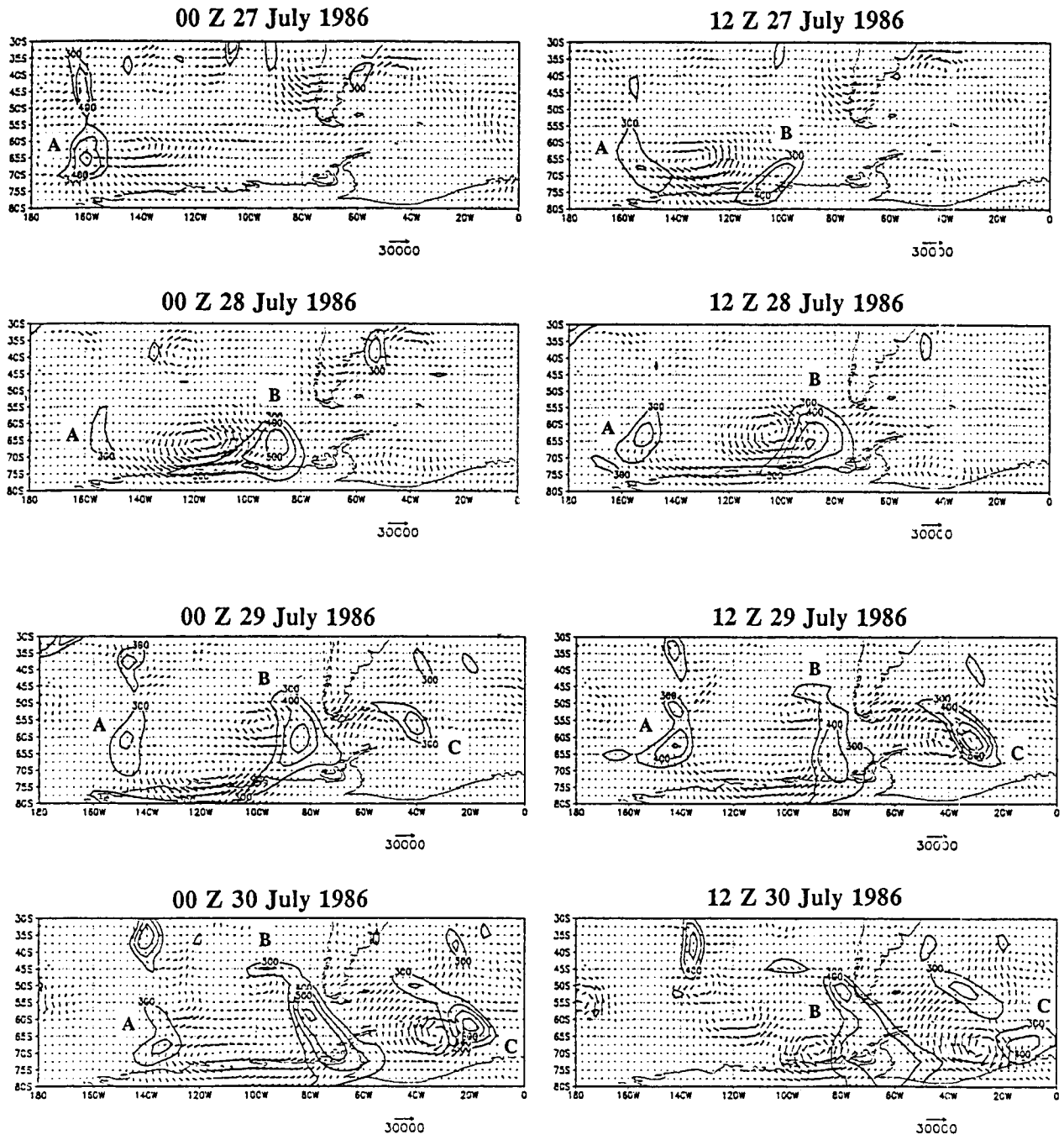

Fig. 5. Sequence, at 12-h intervals, of the vertically averaged (50 hPa to 1000 hPa) eddy kinetic energy, K_e, and ageostrophic geopotential flux vectors $(v\phi)_a$. Contours are drawn at 100 m^2s^2 interval, starting at 300 m^2s^2.

The sequence clearly reflects the closed connection between the eddy energy centers and the energy fluxes associated with the downstream development. At 00Z 27 July, an energy center on the eastern side of a preexisting trough centered at 170°W, hereafter center A, seems to begin its decaying stage, with strong divergent geopotential fluxes downstream. These fluxes emanating from the energy center A, intensify 12 and 24 hours later and are strongly convergent on the eastern side of the blocking anticyclone. A new energy center, center B, intensifies on the western side of the developing trough over the Drake Passage. At 12Z 28 July energy center B shows convergent fluxes on its upstream side and divergent fluxes are beginning to develop on its downstream side, though the net effect of these fluxes is convergence. By 00Z 29 July energy center B has moved northeastward, stops growing and divergent fluxes downstream become stronger than convergent fluxes upstream. Fluxes emanating from energy center B become convergent on the eastern side of the developing trough, over the western Atlantic Ocean where the strengthening of another energy center, center C, takes place. By this time, the initial strengthening of the developing cyclone over the Atlantic Ocean is apparent (see Fig. 4). The growing energy center C is fed, during the next 12 and 24 hours, by fluxes emanating from the upstream decaying center B, which still receives energy from the original center A, dissipated by 12Z 30 July. By 00Z 30 July energy center C seems to split and energy fluxes recirculate around the mature cyclone over the Weddell Sea. 12 hours later the southern tip of the energy center begins its dissipation while the northern part, which still receives energy via geopotential fluxes from the decaying center B, tends to undergo further intensification.

The picture described fits quite well with the downstream development concept discussed by O&K and O&S as there is an eastward propagation of energy in which each energy center intensifies through the influx of energy and decays as the energy is radiated downstream.

In an attempt to explain which are the processes that control the eddy kinetic energy evolution of the centers identified, the contribution of the most relevant terms of the eddy kinetic energy budget (eq. 1) throughout the evolution of the cyclonic wave has been evaluated. This methodology allows us to determine sources and sinks associated with eddy kinetic energy patterns.

Figures 6, 7, 8 and 9 show the vertically averaged (50 hPa to 1000 hPa) contributions to this budget for selected dates representative of each stage of evolution for energy centers A, B and C. The vertical average of the term that represents the vertical divergence of eddy kinetic energy flux and the vertical flux divergence are not presented, as their contributions are small. The tendency of the eddy kinetic energy has not been calculated, because only 12 hours interval information is available and a time difference using this data would give unreliable results. The figures show the terms that contribute significantly to the energy budget: convergence of advected fluxes, $\nabla\bullet(V\text{Ke})$, and the main contributors to the advection of geopotential heights, the convergence of ageostrophic geopotential flux, $-\nabla\bullet(v\phi)_a$, and the baroclinic conversion, $-\omega\alpha$. In order to identify the energy centers, contours of eddy kinetic energy are superimposed. Light and dark shading indicate values between 300 and 400 m^2s^{-2}, and between 500 and 600 m^2s^{-2}, respectively.

In Figure 6, which corresponds to the 12Z 27 July analysis, it can be noted that the term $-\nabla.(v\phi)_a$ contributes to the dissipation of energy center A. Baroclinic conversion, $-\omega\alpha$, associated to the warmer ascending air on the eastern side of the western trough, constitutes a source of eddy kinetic energy. This generation of energy is overcome by divergence of ageostrophic geopotential fluxes and, in consequence, the system decays.

Although the contribution of the term $-\nabla.(V\text{Ke})$ is more intense locally, positive values upstream and negative values downstream are nearly compensated. This term is a good indicator of where is the energy center being displaced and indicates that energy center A is moving mainly southeastward, while it radiates energy further eastward.

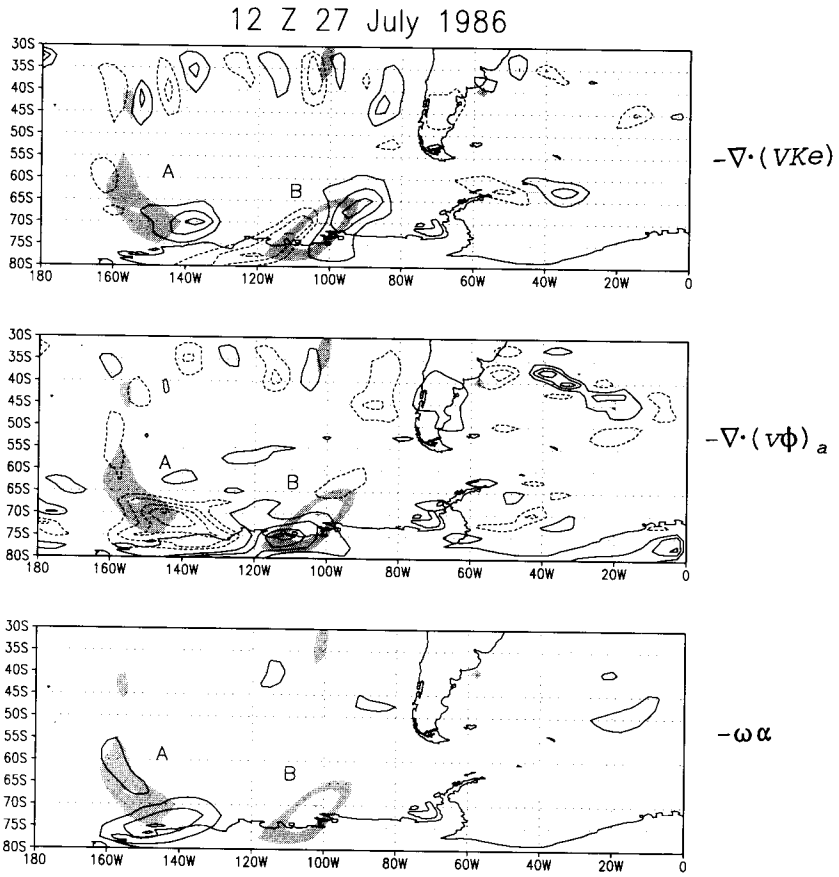

Fig. 6. Energetic at 12 Z 27 July 1986. Top panel: vertically averaged eddy kinetic energy, K_e, and convergence of eddy kinetic energy fluxes, $-\nabla(VK_e)$. Second panel: vertically averaged eddy kinetic energy and ageostrophic geopotential flux convergence, $-\nabla(v\phi)_a$. Bottom panel: vertically averaged eddy kinetic energy and baroclinic generation, $-\omega\alpha$. For all the panels: contours are drawn every 0.005 m^2s^{-3}. The zero contour is omitted for clarity, solid contours are positive, and dashed contours negative. Light and dark shading indicate K_e values between 300 and 400 m^2s^{-2} and between 500 and 600 m^2s^{-2}, respectively.

Energy center A loses energy via geopotential fluxes through the ridge toward the entrance region of the new center, B, which is beginning to grow on the western side of the developing trough. These fluxes continue strengthening for another 12-24 hours, and are the dominant energy source for the center B. At 12Z 28 July (Fig. 7), energy center B is advected northeastward, as evident from $-\nabla.(VKe)$, and continues to grow due to strong convergence of geopotential fluxes on its upstream end, while radiates energy, via $(v\phi)_a$, over the eastern side of the Drake Passage. These fluxes become convergent in a region located 15°-20° downstream, on the eastern side of the trough, where the new energy center C is undergoing its initial development. The baroclinic term constitutes a very weak source of energy for center B, which is developing in a region of relative low baroclinicity, downstream the end of the sub-polar jet, as shown in Figure 3d.

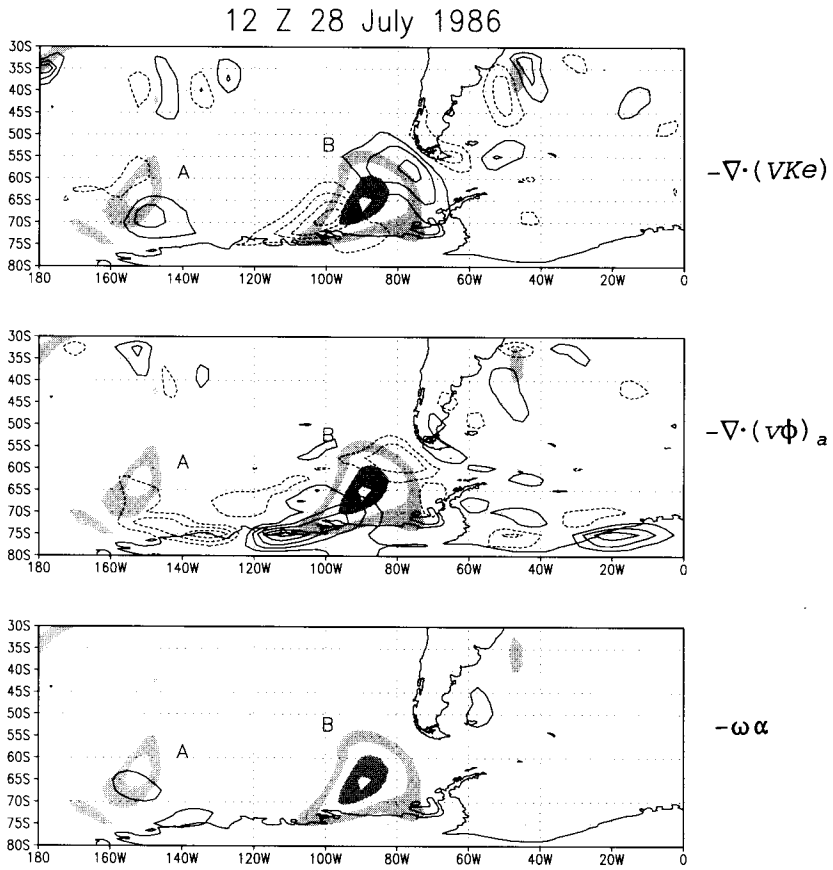

Fig. 7. Same as Fig. 6, but for 12 Z 28 July 1986.

By 12Z 29 July (Fig. 8), which is the time when the surface cyclone located to the north of the Weddell Sea is undergoing its strong deepening, energy center C shows a great growth, while energy center B begins its decaying stage. At this time energy center B still receives energy via ageostrophic flux convergence from the upstream energy center A, but it also radiates energy downstream, though the net effect is divergence. Divergent fluxes out of energy center B become convergent in two localized regions on the upstream side of energy center C, which are stronger on its northern tip. The convergence of advected kinetic energy, -∇.(VKe), also shows two pairs of divergence-upstream/ convergence-downstream maxima. During this time energy center C grows also due to baroclinic conversion, associated to ascending warm air ahead of the trough. As a consequence of the double structure of convergence / divergence of both, the energy fluxes and the ageostrophic fluxes noted in Fig. 8, the center C splits. This behavior is evident 24 hours later, as shown in Figure 9.

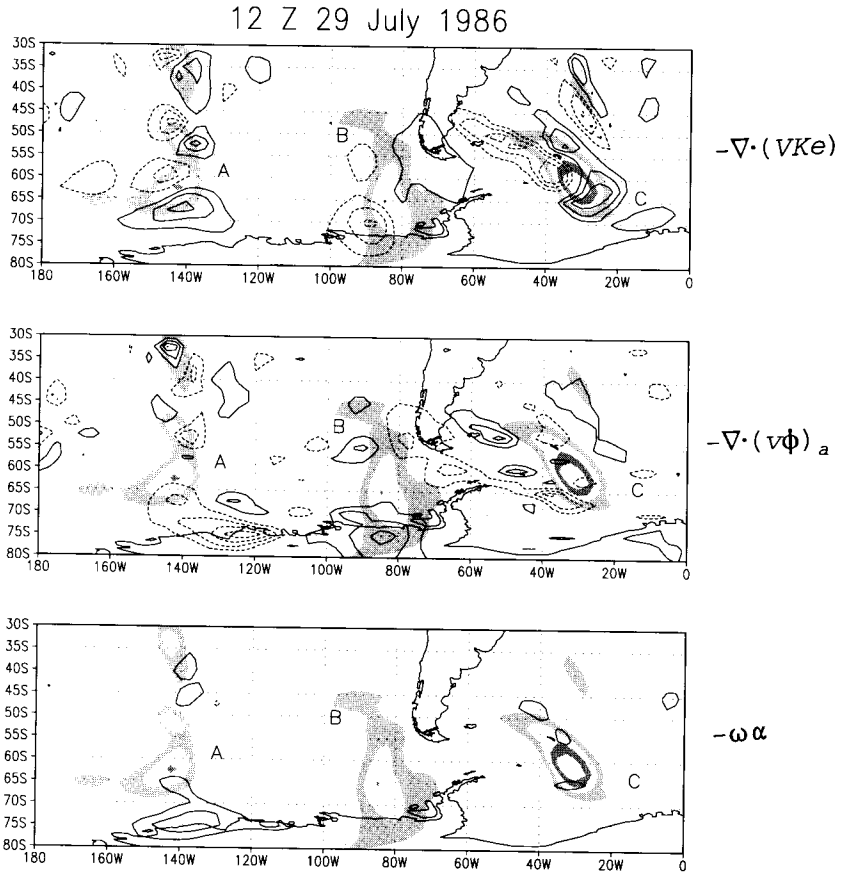

Fig. 8. Same as Fig. 6, but for 12 Z 29 July 1986.

By 12Z 30 July (Fig. 9), at the time when the surface cyclone over the Weddell Sea begins its dissipation, the southern part of the center C weakens and is displaced southeastward. During this time, ageostrophic fluxes tend to recirculate around the axis of the cyclone, with strong ageostrophic fluxes out of the energy center. Baroclinic contribution, associated with the topographic slope over the Antarctic coast, is positive, although much weaker. The northern part of energy center C continues to be fed by the upstream decaying center B and tends to be advected northeastward, far from the deep surface cyclone. The pattern of convergence of ageostrophic fluxes upstream and divergent ageostrophic fluxes downstream contributes to the development of a new energy center further downstream, over the Atlantic Ocean, as evident in the Hovmöller diagram in Figure 2.

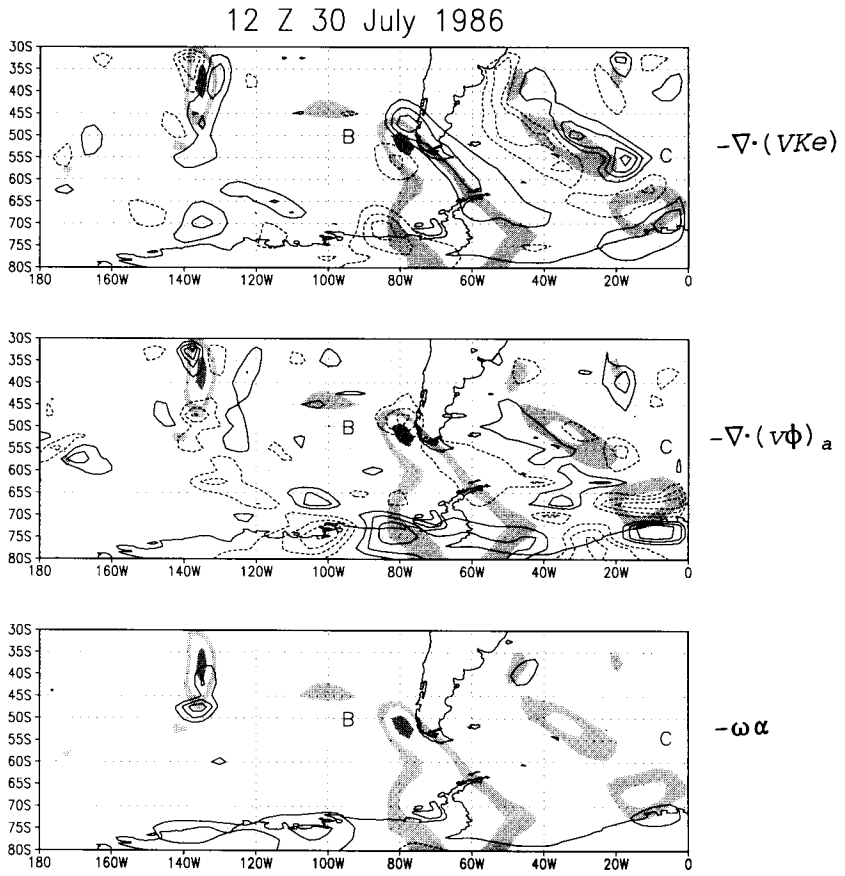

Fig. 9. Same as Fig. 6, but for 12 Z 30 July 1986.

5. Summary and conclusions

In this paper an individual case of cyclone wave at the high southern latitudes has been studied. Our main objective is to achieve a better understanding of some basic mechanisms that contribute to its development. The eddy kinetic energy budget was evaluated, using 12-h ECMWF analysis, in order to diagnose and quantify the roles of the energy fluxes and baroclinic conversion in their evolution. The ridge-trough system that was the subject of this work occurred on the periphery of the Antarctic plateau, between the eastern end of the polar jet over the South Pacific and the Weddell Sea region, on 26-30 July 1986. During this period, a blocking anticyclone over the eastern South Pacific ocean is followed by a deep trough in the Drake Passage region.

At the initial state the South Pacific was dominated by a deep trough near 170°W, an incipient trough over the Bellinghausen Sea, and an amplifying ridge located between them. An eddy kinetic energy center associated with the western trough was losing energy mainly via ageostrophic geopotential fluxes, which were strongly convergent ahead of the ridge axis. As a consequence, a new energy center grew to the west of the Drake Passage, in a region of weak to moderate low-level baroclinicity. As the trough developed over the Antarctic Peninsula, this energy center intensified, moved northeastward and exported energy to the eastern side of the trough. Another

energy center developed to the east of the Drake Passage downstream of the trough. By this time occurred the development of a cyclone over the Southwestern Atlantic. During the next hours, the cyclone intensified and moved toward the Weddell Sea, where it became nearly stationary. The storm was accompanied by the eastern energy center, which continued to grow, while that on the western side of the trough began its decaying stage. At the final state, the eastern center splitted in two maxima. The net effect on the southern center, associated with the cyclone over the Weddell Sea, was loss of energy (positive contribution through baroclinic conversion weaker than negative contribution through divergence of ageostrophic geopotential fluxes). The northern center developed ageostrophic and advected fluxes with an equatorward component in the South Atlantic region.

In general, the stages of development of this ridge-trough system fit quite well the conceptual picture of "downstream baroclinic evolution" described by Orlanski and Sheldon (1995). In that paper they presented a case study (the USA "Blizzard of '93") in which the evolution of the trough associated with the Blizzard is dominated, during the early stages of evolution, by the geopotential fluxes, though the explosive growth of the system is due to vigorous baroclinic conversion. In contrast, in the case study presented on this paper, the role of the baroclinic conversion is not so relevant in the development of the energy centers.

Besides these physical processes linked with the internal dynamic of the atmosphere other possible factors, such as the orographic and surface forcing, could affect the cyclogenesis and cyclolysis in this region. In the SH the intense climatological sub-antarctic trough (associated with the high density of cyclonic systems) is in the same region of the sea ice zone. Sea ice plays a modifying role in the nature of air-sea interaction, and it would be expected to have an influence on synoptic processes and also atmospheric climate in these regions.

It has been suggested that the high-latitude distribution of cyclogenesis and cyclolysis and the variability of cyclone frequency would also be related to the topography of the Antarctic landmass (Taljaard 1967, Mechoso 1980, Carleton 1992). In particular, the Andes and the Antarctic Peninsula constitute a mountain barrier which can modify the large-scale flow within the cyclones form. The embayments and promontories in the Antarctic coastline, the persistent katabatic wind regime and the slopes of the Antarctic plateau are all factors that could affect cyclogenesis and cyclolysis in the region. The impact of these forcings in the life cycle of subantarctic cyclones is not thoroughly understood and, therefore, they would have to be investigated in future projects.

Acknowledgements

The authors wish to thank Dr. Isidoro Orlanski for valuable discussions and to the anonymous reviewer whose comments contributed to its readability and clarity. This work has been partially supported by the European Commission under contract CEE C11-CT94-0111.

REFERENCES

Alessandro, A. P. and R. E. Lichtenstein, 1996. Anomalías persistentes de la circulación atmosférica durante la sequía del invierno de 1995. VII Congreso Latinoamericano e Ibérico de Meteorología, Bs. As., 315-316.

Berbery, H. and C. Vera, 1996. Characteristics of the Southern Hemisphere winter storm track with filtered and unfiltered data. *J. Atmos. Sci.* **53**, 468-481.

Carleton, A. M., 1981. Monthly variability of satellite-derived cyclonic activity for the southern hemisphere winter. *J. Climatol.*, **1**, 21-38.

Carleton, A. M., 1992. Synoptic interactions between Antarctica and lower latitudes. *Aust. Meteor. Mag.* **40**, 129-147.

Cressman, G. P., 1948. On the forecasting of long waves in the upper westerlies. *J. Meteor.* **4**, 999-1015.

Chang, E. K. M., 1993. Downstream development of baroclinic waves as inferred from regression analysis. *J. Atmos. Sci.* **50**, 2038-2053.

Chang, E. K. M. and I. Orlanski, 1993. On the dynamics of a storm track. *J. Atmos. Sci.* **50**, 999-1015.

Garreaud, S. R., 1994. Configuraciones atmosféricas regionales durante grandes tormentas pluviales en Chile central. *Meteorologica*, **19**, 73-81.

Hovmöller, E., 1949. The trough-and-ridge diagram. *Tellus* **1**, 62-66.

Hoskins, B. J. and P. J. Valdes, 1990. On the existence of storm-tracks. *J. Atmos. Sci.* **47**, 1854-1864.

Joung, C. H. and M. H. Hitchman, 1982. On the role of successive downstream development in East Asian polar outbreaks. *Mon. Wea. Rev.* **110**, 1224-1237.

Leighton, R. M.,1994. Monthly anticyclonicity and cyclonicity in the Southern Hemisphere; averages for January, April, July, and October. *Int. J. Climatol.*, **14**, 33-45.

Mayes, P. R., 1985. Secular variations in cyclone frequencies near the Drake Passage, southwest Atlantic. *J. Geophys. Res.*, **90**, 5829-5839.

Mechoso, C. R., 1980. The atmospheric circulation around Antarctica: Linear stability and finite amplitude interactions with migrating cyclones. *J. Atmos. Sci.* **37**, 2209-2233.

Namias, J. and P. F. Clapp, 1944. Studies of the motion and development of long waves in the westerlies. *J. Meteor.* **1**, 57-77.

Orlanski, I. and E. K. M. Chang, 1993. Ageostrophic geopotential fluxes in downstream and upstream development of baroclinic waves. *J. Atmos. Sci.* **50**, 212-225.

Orlanski, I. and J. Katzfey, 1991. The life cycle of a cyclone wave in the Southern Hemisphere. Part I: Eddy energy budget. *J. Atmos. Sci.* **48**, 1972-1998.

Orlanski, I., J. Katzfey, C. Menéndez, M. Marino, 1991. Simulation of an extratropical cyclone in the Southern Hemisphere: model sensitivity. *J. Atmos. Sci.* **48**, 2293-2311.

Orlanski, I. and J. Sheldon, 1993. A case of downstream baroclinic development over western North America. *Mon. Wea. Rev.* **121**, 2929-2950.

Orlanski, I. and J. Sheldon, 1995. Stages in the energetics of baroclinic systems. *Tellus* **47A**, 605-628.

Simmons, A. J. and B. J. Hoskins, 1979. The downstream and upstream development of unstable baroclinic waves. *J. Atmos. Sci.* **37**, 1679-1684.

Sinclair, M. R., 1994. An objective cyclone climatology for the Southern Hemisphere. *Mon. Wea. Rev.* **122**, 2239-2256.

Taljaard J., J., 1967. Development, distribution and movement of cyclones and anticyclones in the Southern Hemisphere during the IGY. *J. Appl. Meteorol.* **6**, 973-987.

Trenberth, K. E., 1986. The signature of a blocking episode on the general circulation in the Southern Hemisphere. *J. Atmos. Sci.* **43**, 2061-2069.

van Loon, H., 1965. A climatological study of the atmospheric circulation in the Southern Hemisphere during IGY. Part I; July 1957-31 March 1958. *J. Appl. Meteor.* **4**, 479-491.